

## Generation of Polarization-entangled Photon Pairs in 1.5- $\mu\text{m}$ Telecommunication Band

*Hiroki Takesue*<sup>†</sup>

### Abstract

The generation of entangled photon pairs in the 1.5- $\mu\text{m}$  telecommunication band is an important technique for making fiber-based quantum information systems such as quantum key distribution and quantum repeater systems. This paper reviews two experiments that were conducted by NTT. The first was based on spontaneous four-wave mixing in a dispersion-shifted fiber loop. This configuration made it possible to generate polarization-entangled states very stably. The second experiment used spontaneous parametric down-conversion in a periodically poled lithium niobate waveguide and an orthogonal polarization delay circuit. In both experiments, we obtained two-photon interference with sufficient visibility for us to observe a violation of Bell's inequality.

### 1. Introduction

The entangled states of quantum particles [1] are the quintessential feature of quantum mechanics because they highlight its non-locality most vividly [2]. Moreover, entanglements form the basis of quantum information and facilitate applications such as quantum cryptography, quantum teleportation, and quantum computation [3]. Of the many forms of entanglement, entangled photons are important because they are suitable for distributing quantum information over long distances. The generation of entangled photons in the 1.5- $\mu\text{m}$  telecommunication band is especially important for quantum information systems over optical fiber networks, so some pioneering research groups, including that of my coworkers and I, have recently started studying this issue. This paper reviews our two recent experiments on the generation of polarization-entangled photon pairs in the 1.5- $\mu\text{m}$  band. The first experiment was based on spontaneous four-wave mixing (SFWM) in a fiber loop formed with a polarization beam splitter (PBS) and a dispersion-shifted fiber (DSF) [4]. The fiber-loop configuration enabled, polarization-entangled states to be generated much more stably in our

experiment than in a previously reported experiment using SFWM [5]. The second experiment used spontaneous parametric down-conversion (SPDC) in a periodically poled lithium niobate (PPLN) waveguide. Although SPDC is a commonly used approach for generating entangled photons, we combined it with our method for converting time-bin entanglement to polarization entanglement [6], which has the advantage of being applicable to a nonlinear medium with polarization dependence such as PPLN.

### 2. Entangled photon pair

We consider two photons that constitute one system. When the state of a two-photon system cannot be written as the product of the state of each photon, the two-photon system is called an entangled photon pair [1]. Here, we call one photon of the pair the signal photon and the other the idler photon. There are several kinds of entangled photon pairs based on different variables: here, as an example, we treat polarization entanglement. An example of a polarization-entangled state is given by

$$|\Phi^+\rangle = \frac{1}{\sqrt{2}}(|H\rangle_s|H\rangle_i + |V\rangle_s|V\rangle_i), \quad (1)$$

where  $|H\rangle_x$  and  $|V\rangle_x$  denote the horizontal (H) and vertical (V) polarization states, respectively, of  $x = s$  (signal) or  $i$  (idler) photons. We now consider the

<sup>†</sup> NTT Basic Research Laboratories  
Atsugi-shi, 243-0198 Japan  
E-mail: htakesue@will.brl.ntt.co.jp

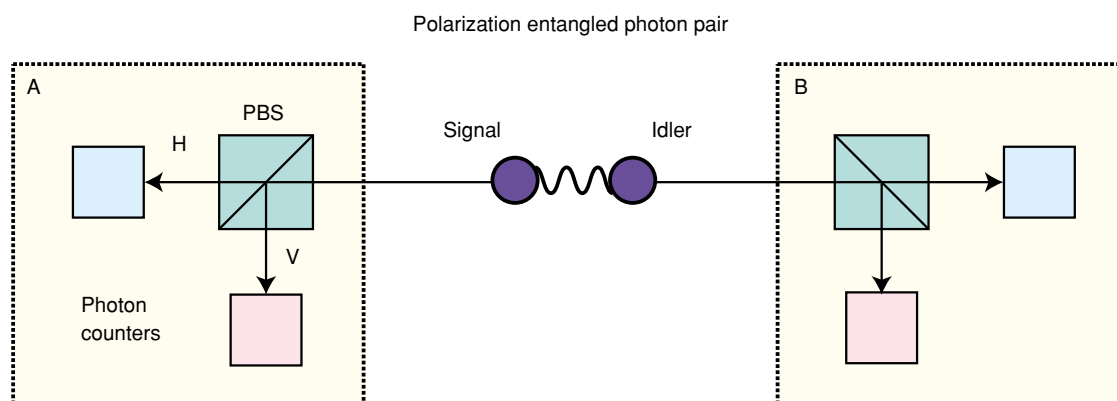


Fig. 1. Coincidence measurement of polarization-entangled photon pair.

coincidence measurement shown in **Fig. 1**. Signal and idler photons are separated and sent to observers A and B, respectively. Each observer is equipped with a PBS followed by two photon counters, which enable the observer to determine whether the polarization of an incoming photon is H or V. Equation (1) implies that the outcome of the polarization measurement undertaken by each observer is completely random, which means that each photon is depolarized. However, if observers A and B undertake the same measurement for many entangled photon pairs whose states are given by Eq. (1) and disclose their outcomes to each other, they will find that their outcomes are always correlated: if the signal photon is measured and found to be in the H (V) polarization state, the idler is also in the H (V) polarization state.

A similar situation could be achieved using the following approach, which does not use an entangled state such as Eq. (1). We prepare many sets of two photons and apply random polarization modulation to both so that the polarizations of the two photons in each set become either H or V with equal probability. Then, if two observers undertake a measurement to distinguish H or V polarization, they will see the same result as above. However, with this “photon-pair” source, the correlation vanishes if the observers measure their respective photons using PBSs that distinguish  $+45^\circ$  and  $-45^\circ$  diagonal polarizations (which can be achieved simply by rotating the PBS by  $45^\circ$  around the light axis).

On the other hand, if they undertake a measurement that distinguishes  $\pm 45^\circ$  diagonal polarizations for the entangled state shown by Eq. (1), they obtain different results, as explained in the following.  $|H\rangle_x$  and  $|V\rangle_x$  can be rewritten using the  $+45^\circ$  diagonal polarization state  $|D^+\rangle_x$  and the  $-45^\circ$  diagonal polarization

state  $|D^-\rangle_x$  as  $|H\rangle_x = \frac{1}{\sqrt{2}}(|D^+\rangle_x + |D^-\rangle_x)$  and  $|V\rangle_x = \frac{1}{\sqrt{2}}(|D^+\rangle_x - |D^-\rangle_x)$ , respectively. By using the above equations, we can express Eq. (1) as

$$|\Phi^+\rangle = \frac{1}{\sqrt{2}}(|D^+\rangle_s |D^+\rangle_i + |D^-\rangle_s |D^-\rangle_i). \quad (2)$$

Equation (2) shows that the correlation between measurement outcomes for the signal and idler photons is still preserved even if the observers measure the photon pairs using different measurement bases. The above argument reveals a peculiar characteristic of quantum entanglement: although the polarization of each photon is undetermined, the relationship between the polarizations of the two photons is fixed, regardless of the measurement basis.

The “quantum correlation” between signal and idler photons is preserved even if they are separated by a macroscopic distance. This means that, for example, when the signal photon is measured and found to be in the H polarization state, the polarization state of the idler photon becomes H at the moment of signal photon measurement, even if they are separated by, say, hundreds of kilometers. This non-locality predicted by quantum mechanics was criticized by Einstein as an example of the incompleteness of quantum mechanics, and it generated considerable argument among physicists [2]. This argument ended after Bell proposed an inequality to test the validity of local realistic theories [7] and subsequent experiments were undertaken that supported quantum mechanics [8].

Recently, a practical entangled photon-pair source was developed in the short-wavelength band (around

0.7–0.8 μm) [9], and it has been playing an important role in many quantum information experiments. However, we need an entangled photon-pair source for the 1.5-μm band if we are to make practical quantum communication systems over optical fiber networks. The following sections describe experiments in which we generated polarization-entangled photon pairs in the 1.5-μm band.

### 3. Polarization entanglement generation using SFWM in a fiber loop

#### 3.1 Generation scheme

Most entangled photon-pair sources have two functions. The first is to generate quantum-correlated photon-pair states such as  $|H\rangle_s|H\rangle_i$  and  $|V\rangle_s|V\rangle_i$ . Most previous experiments used SPDC in a second-order optical nonlinear medium to obtain such states. The second function is to superpose these photon-pair states and create a state such as Eq. (1). In our experiment, the photon-pair states were generated using SFWM in a DSF, and they were superposed using a fiber-loop configuration.

SFWM is a third-order optical nonlinear process in which two pump photons are annihilated and a signal-idler photon pair is generated. Here, we consider a partially degenerate case in which the optical frequencies of the two pump photons are the same. Then, the angular frequencies of the pump, signal, and idler photons  $\omega_p$ ,  $\omega_s$ , and  $\omega_i$ , respectively, satisfy the following relationship.

$$2\omega_p = \omega_s + \omega_i \quad (3)$$

This energy conservation rule indicates that the signal

and idler photons must be created at the same time instance (time correlation).

We use a single-mode fiber as a nonlinear medium. A single-mode fiber exhibits slight birefringence caused by small deviations from cylindrical geometry or small fluctuations in material anisotropy. Moreover, in a long fiber, the principal axis changes randomly along the fiber due to external perturbations, such as microbending and local pressure. In such fibers, only signal and idler photons whose polarization states are the same as those of the pump photons are generated [10]. Therefore, for example, if we input pump photons with a horizontal polarization into a fiber, we can obtain a polarization-correlated photon-pair state  $|H\rangle_s|H\rangle_i$  through a spontaneous FWM process.

When the power-dependent change of refractive index is negligible, photon pairs are generated efficiently with the following phase-matching condition satisfied.

$$2k_p = k_s + k_i \quad (4)$$

Here,  $k_p$ ,  $k_s$ , and  $k_i$  denote the wavenumbers of the pump, signal, and idler photons, respectively. We can achieve this condition in the 1.5-μm band by using a DSF and setting the pump wavelength at the zero-dispersion wavelength. Thus, the DSF enables us to generate photon pairs effectively in the 1.5-μm band.

To generate a polarization-entangled state, we place the DSF in a loop configuration with a PBS, as shown in Fig. 2. A pump pulse with a +45° diagonal polarization state is input into the fiber loop. The PBS divides the pump pulse into horizontal and vertical polarization components of equal power. The H and

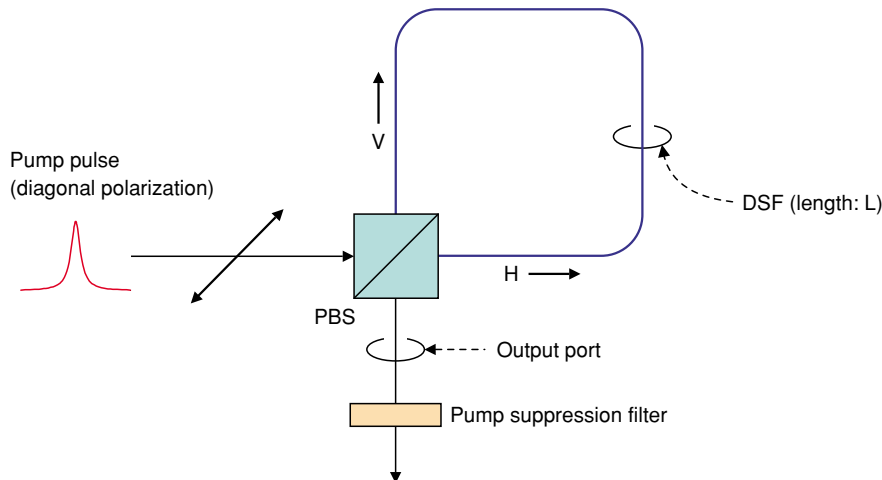


Fig. 2. Schematic diagram of our method.

V components generate signal-idler photon pairs  $|H\rangle_s|H\rangle_i$  and  $|V\rangle_s|V\rangle_i$  while propagating in the loop in the counter-clockwise and clockwise directions, respectively. The photon pairs then move to the output port of the PBS. With an appropriate pump power, we can make the probability of generating two pairs simultaneously very low. As a result, a superposed state of the two product states  $|H\rangle_s|H\rangle_i$  and  $|V\rangle_s|V\rangle_i$  is output from the PBS. After eliminating the pump light using an optical filter, we can obtain a polarization-entangled state.

For a maximally entangled state, the relative phase between  $|H\rangle_s|H\rangle_i$  and  $|V\rangle_s|V\rangle_i$  should be 0 or  $\pi$  at the loop output. With  $\Delta n$  denoting the difference between the DSF refractive indices for the H and V components, the state output from the fiber loop is expressed as

$$|\Phi^+\rangle = \frac{1}{\sqrt{2}} \left( |H\rangle_s|H\rangle_i + \exp\left(2i\frac{\omega_p\Delta nL}{c}\right) |V\rangle_s|V\rangle_i \right), \quad (5)$$

where  $L$  is the fiber length. Therefore, if the fiber is short or the birefringence is small, the condition for the maximally entangled state can be automatically achieved. Note that this relative phase is very stable without any feedback control because H and V polar-

ization components propagate in the common path.

### 3.2 Experiment

We performed an experiment to test the effectiveness of our method using the setup shown in Fig. 3. Pump pulses with a width of 20 ps and repetition frequency of 2 GHz were generated using a gain-switched semiconductor laser. The center wavelength of the pulses was set at 1551 nm, namely, close to the zero-dispersion wavelength of the DSF used in the experiment. The pump pulses were input into an optical intensity modulator, which reduced the repetition frequency to 100 MHz, and were amplified using an erbium-doped fiber amplifier (EDFA). The amplified spontaneous emission noise in the EDFA output was eliminated using narrowband fiber-Bragg gratings (FBGs) and optical circulators cascaded in pairs. The polarization state of the pulses was adjusted to 45° linear polarization using a polarization controller (a quarter-wave plate (QWP) combined with a half-wave plate (HWP)) and a polarizer. Then the pulses were launched into the loop, which consisted of a PBS, a 2.5-km DSF, and two polarization controllers. The peak power of the pump pulse was 42 mW at the input of the DSF. We adjusted the polarization con-

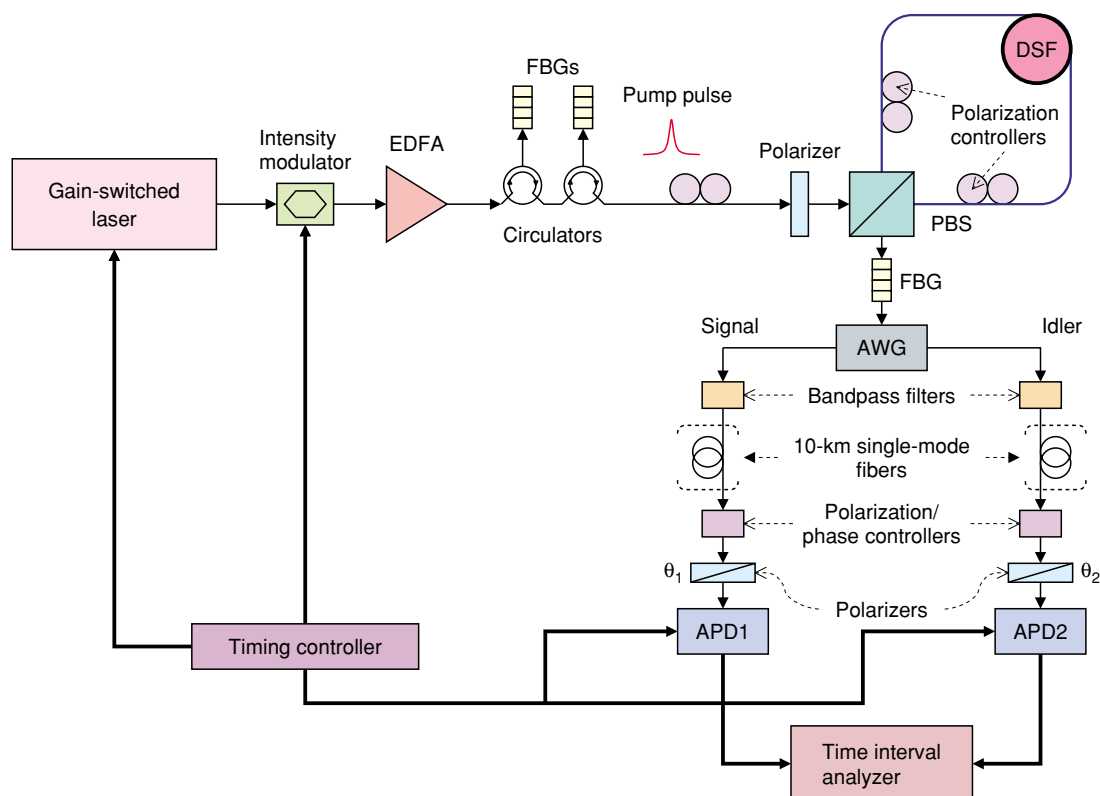


Fig. 3. Experimental setup.

trollers in the loop so that the generated photon pairs were properly output from the loop. The output photons from the loop were input into narrowband FBGs to suppress the pump photons and were then launched into an arrayed waveguide grating (AWG) with a 50-GHz channel spacing to separate the signal and idler photons. AWG output channels with peak wavelengths of 1552.7 and 1549.4 nm were used for the signal and idler, respectively. The output photons from the AWG were filtered using dielectric optical bandpass filters to further suppress the pump photons. The FBGs, AWG, and bandpass filters suppressed the pump photons by  $>125$  dB relative to the signal and idler photons. The 3-dB bandwidths of the signal and idler were both approximately 25 GHz. This value was limited mainly by the width of the AWG passband.

The output photons from each bandpass filter were then input into a polarization/phase controller, which consisted of a QWP, an HWP, and a Babinet-Soleil compensator. Here, the polarization states of the signal and idler photons were adjusted so that the two photons experienced the same polarization change after they were separated by the AWG. Each photon was then input into a rotatable polarizer and detected with an avalanche photodiode (APD) operated in a gated Geiger mode. The electrical signals from the APDs were input into a time interval analyzer for coincidence measurements. In the time interval analysis, we measured coincidences in matched and un-matched slots. A coincidence in a matched slot is

a “true” coincidence, which we define as a coincidence caused by photons generated by the same pump pulse. Please note that our definition means that “true” coincidences include accidental coincidences such as those caused by photons from two different pairs generated with the same pump pulse or by noise photons generated with the same pump pulse. A coincidence in an un-matched slot corresponds to an accidental coincidence caused by photons generated by different pump pulses. These appear at different time instances separated by the detector gate period. Since the average coincidence rate in an un-matched slot is the same as the average accidental coincidence rate in a matched slot, we can estimate the number of accidental coincidences in a matched slot by measuring the coincidences in an un-matched slot. The quantum efficiency, gate width, and repetition frequency of the APDs were 10%, 2.5 ns, and 1 MHz, respectively. The dark count probabilities per gate were  $2.5 \times 10^{-5}$  for APD1 (for signal) and  $4 \times 10^{-5}$  for APD2 (for idler). The photon pair production ratio per pump photon was approximately  $6 \times 10^{-10}$ , and the average count rates for the signal and idler were 490 and 380 counts per second, respectively. Note that the whole system was constructed with fiber connections, so it was very stable.

We rotated the angle of the polarizer for the signal  $\theta_1$  while fixing that for the idler  $\theta_2$  at  $0^\circ$  and measured the coincidence rate  $C(\theta_1, \theta_2)$ . The results are shown by the circles in **Fig. 4(a)**. The horizontal axis shows the  $\theta_1$  value, and the vertical axis shows the coinci-

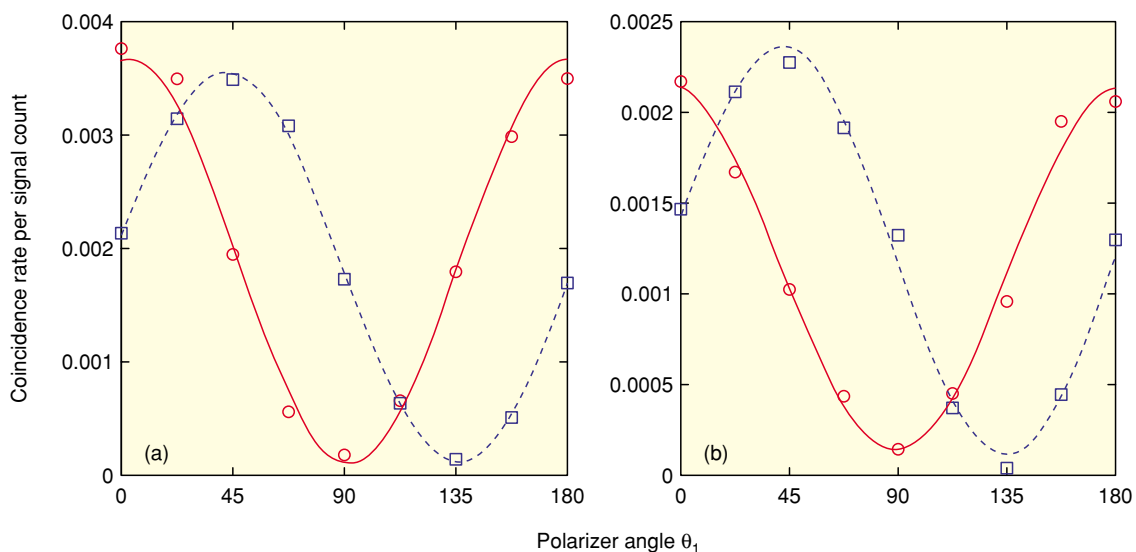


Fig. 4. (a) Coincidence rate per signal count as a function of  $\theta_1$ . (b) Coincidence rate per signal count as a function of  $\theta_1$  after the signal and idler photons had been separated by 20 km of optical fiber. Circles:  $\theta_2 = 0^\circ$ , squares:  $\theta_2 = 45^\circ$ .

dence rate per signal count. Here, accidental coincidence counts were subtracted from the coincidence counts in a matched slot when calculating the coincidence rate. As a result, a coincidence fringe with a visibility of 94.2% was obtained. To confirm the quantum correlation, we performed the same experiment for  $\theta_2 = 45^\circ$ . As shown by the squares in Fig. 4(a), we obtained a coincidence fringe with 91.2% visibility. From these results, we conclude that our method successfully generated polarization-entangled photon pairs. The phase relationship between the two coincidence curves indicated that the obtained

state was  $|\Phi^+\rangle = \frac{1}{\sqrt{2}}(|H\rangle_s|H\rangle_i + |V\rangle_s|V\rangle_i)$ . The high

visibility indicated that the birefringence of the DSF (i.e.,  $\Delta n$ ) was so small that we could make the relative phase in Eq. (5) nearly zero.

When the accidental coincidence counts were included, the visibilities were 77.3 and 77.0% for  $\theta_2 = 0^\circ$  and  $45^\circ$ , respectively. There were several reasons for these accidental coincidence counts. They occurred when two pairs were generated by a pump pulse. In addition, noise photons were probably generated in the DSF through spontaneous Raman scattering. These noise photons may also have caused the accidental coincidence.

We then performed a test of Bell's inequality. We measured the coincidence rate for 16 combinations of polarizer settings ( $\theta_1 = -22.5^\circ, 67.5^\circ, 22.5^\circ, 112.5^\circ$  and  $\theta_2 = -45^\circ, 45^\circ, 0^\circ, 90^\circ$ ) to obtain the  $S$  value of the CHSH (Clauser, Horne, Shimony, and Holt) inequality [7].  $|S|$  should be less than 2 for any local realistic theory. We performed five runs of the  $S$  value measurement and obtained  $S = 2.65 \pm 0.09$  when we subtracted accidental coincidences. Thus, we observed a violation of the CHSH inequality by seven standard deviations. When accidental coincidences were included, the  $S$  value was  $S = 2.06 \pm 0.08$ , which means that we still observed the violation by a 0.75 standard deviation.

Finally, we inserted a 10-km single-mode fiber after the bandpass filter in each path (as shown in Fig. 3), and again measured the coincidence rate as a function of  $\theta_1$  for  $\theta_2 = 0^\circ$  and  $45^\circ$ . The results are shown in Fig. 4(b), where accidental coincidences have been subtracted. The obtained visibilities were 87.2% for  $\theta_2 = 0^\circ$  and 90.1% for  $\theta_2 = 45^\circ$ . Thus, we were able to confirm that the strong quantum correlation between the signal and idler photons was preserved even after they had been separated by 20 km of optical fiber. These results show that polarization-entan-

gled photons generated using our method may be useful for long-distance quantum teleportation, in which a sender and a receiver need to share entangled particles.

#### 4. Polarization-entanglement generation using a PPLN waveguide and an orthogonal polarization delay circuit

##### 4.1 Generation scheme

A PPLN waveguide is a second-order nonlinear medium used in the 1.5- $\mu\text{m}$  band, so it is expected to be another candidate for a quantum-correlated photon-pair source. However, the efficiency of a nonlinear process in a PPLN waveguide is polarization-dependent unlike that in a DSF. This means that the loop configuration described in the previous section cannot be applied to a PPLN waveguide. In the scheme described in this section, we first generate a time-bin entangled state [11] through SPDC in a PPLN waveguide and then convert the time-bin entanglement to polarization entanglement using an orthogonal polarization delay circuit.

We assume that horizontally polarized double pump pulses with a temporal separation of  $\Delta t$  are input into a PPLN waveguide. The coherence time of the pump is larger than  $\Delta t$ . Then, the following time-bin entangled state is created through the SPDC process in the PPLN.

$$|\Phi\rangle = |1,H\rangle_s|1,H\rangle_i + |2,H\rangle_s|2,H\rangle_i \quad (6)$$

In the expression  $|k,A\rangle_x$ ,  $k$  represents the number of time slots (1 or 2),  $A$  denotes the polarization state (H or V), and subscript  $x$  identifies whether the state is the signal (s) or idler (i) state. In Eq. (6), we have omitted an amplitude term that is common to all product states for simplicity. We use the same simplification in subsequent equations in this paper.

This two-photon state with H polarization shown by Eq. (6) is input into the orthogonal polarization delay circuit shown schematically in Fig. 5. The delay circuit consists of a beam splitter (BS), two mirrors, and a QWP. The difference between the round-trip times of the two arms is set to  $\Delta t$ . The optical axis of the QWP is tilted by  $45^\circ$ , so the polarization of the light that makes the round trip of the arm with the QWP is converted into V at the delay circuit output. That is, the delay circuit converts  $|k,H\rangle_x$  to  $|k,H\rangle_x + \exp(i\phi_x)|k+1,V\rangle_x$ , where  $\phi_x = \omega_x\Delta t$  and  $\omega_x$  is either  $\omega_s$  (signal angular frequency) or  $\omega_i$  (idler angular frequency). Then, Eq. (6) is converted to the following state by the delay circuit.

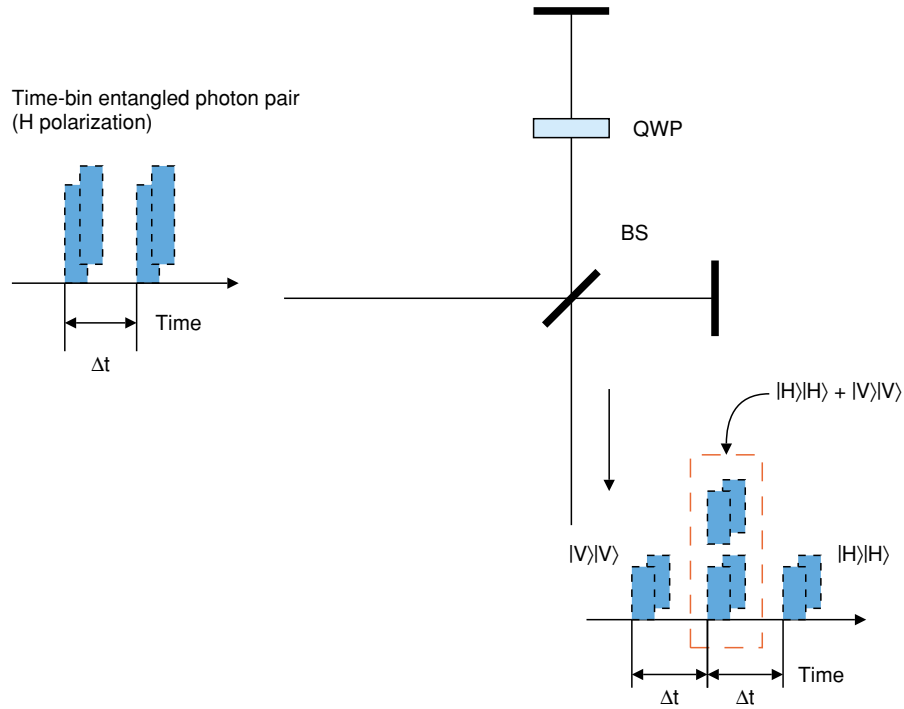


Fig. 5. Schematic diagram of our scheme.

$$\begin{aligned}
 |\Phi\rangle &= (|1,H\rangle_s + \exp(i\phi_s)|2,V\rangle_s) \cdot (|1,H\rangle_i + \exp(i\phi_i)|2,V\rangle_i) \\
 &+ (|2,H\rangle_s + \exp(i\phi_s)|3,V\rangle_s) \cdot (|2,H\rangle_i + \exp(i\phi_i)|3,V\rangle_i) \\
 &= |1,H\rangle_s|1,H\rangle_i + \exp(i\phi_s)|1,H\rangle_s|2,V\rangle_i \\
 &+ \exp(i\phi_s)|2,V\rangle_s|1,H\rangle_i \\
 &+ \exp\{i(\phi_s + \phi_i)\}|2,V\rangle_s|2,V\rangle_i + |2,H\rangle_s|2,H\rangle_i \\
 &+ \exp(i\phi_i)|2,H\rangle_s|3,V\rangle_i \\
 &+ \exp(i\phi_s)|3,V\rangle_s|2,H\rangle_i + \exp\{i(\phi_s + \phi_i)\}|3,V\rangle_s|3,V\rangle_i
 \end{aligned} \quad (7)$$

By post-selecting the coincidence counts in the 2nd time slot, we can extract the 4th and 5th terms. As a result, we can obtain the following polarization-entangled state.

$$|\Phi\rangle = |2,H\rangle_s|2,H\rangle_i + \exp\{i(\phi_s + \phi_i)\}|2,V\rangle_s|2,V\rangle_i \quad (8)$$

## 4.2 Experiment

We experimentally confirmed the feasibility of our method using the setup shown in **Fig. 6**. We used two PPLNs [12]: one (PPLN(1)) for generating 780-nm pump pulses and the other (PPLN(2)) for generating time-bin entangled photons.

A continuous light from an external cavity laser with a wavelength of 1560.0 nm was modulated with an optical intensity modulator to generate double pulses at a repetition rate of 100 MHz. The pulse width, peak power, and temporal separation between the two pulses were 90 ps, 600 mW, and 1 ns, respectively. The coherence time of the laser was approxi-

mately 10  $\mu$ s, so the coherence between the two consecutive pulses was preserved. The pulses were amplified with an EDFA, filtered to reduce the amplified spontaneous emission noise, polarization-controlled, and input into the PPLN(1), where 780-nm double pulses were generated by the second harmonic generation (SHG) process. The output light from PPLN(1) was input into filters that transmitted the 780-nm double pulses while eliminating the remaining 1560-nm light. The peak power of the 780-nm pulse at the filter output was estimated to be 700  $\mu$ W. The 780-nm double pulses were polarization-controlled and then input into PPLN(2), which generated time-bin entangled photons whose state is shown by Eq. (6).

The output from PPLN(2) was polarization-controlled to maximize the number of photons transmitted through a free-space PBS. This PBS was placed in front of an orthogonal polarization delay circuit to ensure that photons with H polarization were launched into the delay circuit. The delay circuit was composed of free-space optics, and one of the mirrors in the delay circuit was mounted on a piezoelectric transducer, which enabled us to adjust the delay time precisely to  $\Delta t$ .

The output from the delay circuit was filtered to suppress the 780-nm pump pulses, and then input into a 3-dB fiber coupler, which separated the signal and

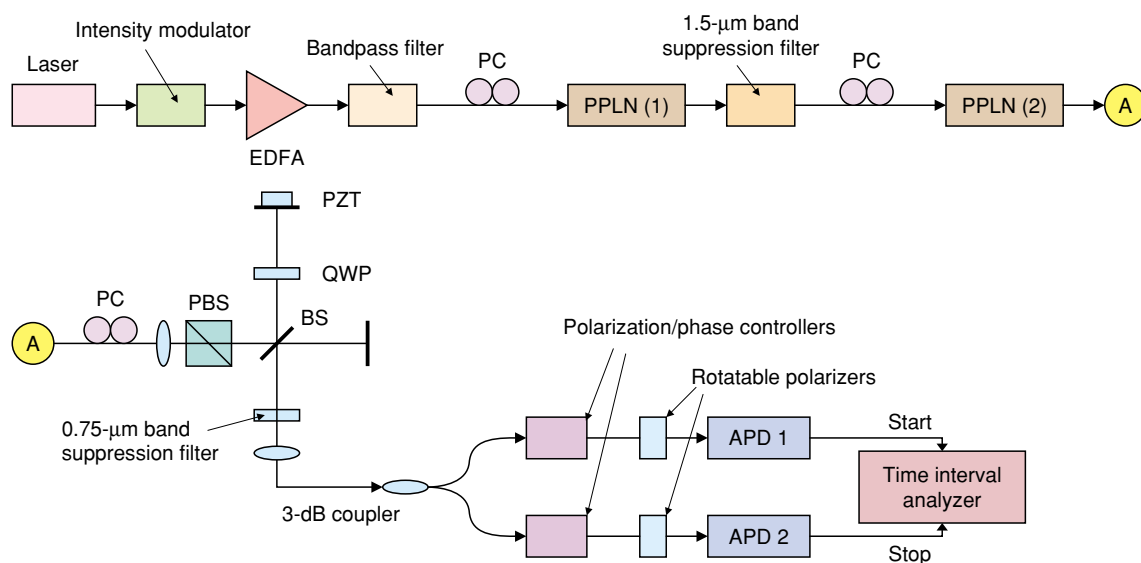


Fig. 6. Experimental setup (PC: polarization controller).

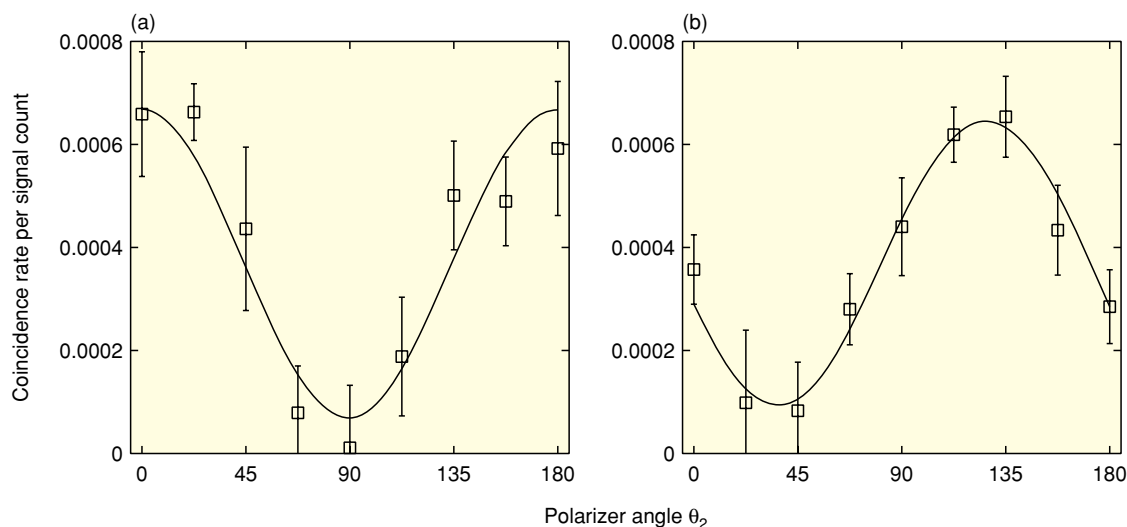


Fig. 7. Coincidence fringes: (a)  $\theta_1 = 0^\circ$  and (b)  $\theta_1 = 45^\circ$ .

idler photons with 50% probability. A photon from each output port of the coupler was input into a polarization/phase controller, which adjusted the polarization states so that both the signal and idler photons experienced the same polarization change after they were separated. Then, each photon was input into a rotatable polarizer and detected with an APD operated in gated Geiger mode with a repetition frequency of 1 MHz. The effective gate widths of the APDs for signal (APD1) and idler (APD2) were 1.3 and 0.5 ns, respectively. The quantum efficiencies of both APDs were 9%. The APDs were triggered in the second time slot in the delay circuit output so that we could

obtain the polarization-entangled state expressed by Eq. (8). The electrical signals from the two APDs were input into a time interval analyzer as start and stop pulses, respectively, for coincidence measurements. The average count rates at the APDs were both about 700 counts per second, and the average number of photons per pulse was estimated to be 0.9. We confirmed that the count rates of both APDs were independent of the polarizer rotation angles.

We rotated the angle of the polarizer in front of APD2,  $\theta_2$ , while fixing that of the one in front of APD1,  $\theta_1$ , to  $0^\circ$  and measured the coincidence rate. The results are shown in Fig. 7(a). The horizontal

axis shows  $\theta_2$  and the vertical axis shows the coincidence rate per signal count. Here, accidental coincidence counts were subtracted. The fitted curve shows the coincidence fringe with a visibility of 82%. To confirm that the above fringe was due to quantum correlation, we then set  $\theta_1$  to  $45^\circ$  and performed the same measurement. As shown in **Fig. 7(b)**, we obtained a coincidence fringe with 74% visibility. These results confirm the polarization entanglement of the signal and idler photons. In addition, these visibilities were large enough to violate Bell's inequality, since a visibility greater than 71% is commonly associated with violation.

Our method has several merits from a practical viewpoint: it can be used with a polarization-dependent nonlinear medium such as PPLN and does not need two nonlinear media with identical characteristics.

## 5. Summary

This paper reviewed two experiments on generating polarization-entangled photons in the 1.5- $\mu\text{m}$  telecommunication band. One was based on spontaneous FWM in a DSF loop. The fiber-loop configuration enabled us to stabilize the relative phase making possible the stable generation of photon pairs. We obtained two-photon interference with visibilities of more than 90% and observed the violation of Bell's inequality by seven standard deviations. We also confirmed that the strong quantum correlation between the photons was preserved after they had been separated by 20 km of optical fiber. The second experiment used SPDC in a PPLN waveguide. Polarization-entangled photons were generated by converting time-bin entanglement to polarization entanglement using an orthogonal polarization delay circuit. We expect these entanglement sources to be key technologies for future quantum information systems implemented over optical fiber networks.

## Acknowledgments

This review paper describes collaborative research conducted with Professor Kyo Inoue of Osaka University and Dr. Masaki Asobe, Dr. Yoshiki Nishida, and Dr. Osamu Tadanaga of NTT Photonics Laboratories. This work was supported in part by the National Institute of Information and Communications Technology (NICT) of Japan.

## References

- [1] F. Morikoshi, "Accessibility between entangled states," NTT Technical Review, Vol. 2, No. 12, pp. 19-25, 2004.
- [2] A. Einstein, B. Podolsky, and N. Rosen, "Can quantum-mechanical description of physical reality be considered complete?" Phys. Rev., Vol. 47, pp. 777-780 (1935); N. Bohr, "Can quantum-mechanical description of physical reality be considered complete?" Phys. Rev., Vol. 48, pp. 696-702 (1935).
- [3] Y. Hirayama, "Quantum information technology," NTT Technical Review, Vol. 1, No. 3, pp. 10-16, 2003.
- [4] H. Takesue and K. Inoue, "Generation of polarization-entangled photon pairs and violation of Bell's inequality using spontaneous four-wave mixing in a fiber loop," Phys. Rev. A, Vol. 70, 031802 (R) (2004).
- [5] X. Li, P. L. Voss, J. E. Sharping, and P. Kumar, "Optical fiber-source of polarization-entangled photons in the 1550 nm telecom band," Phys. Rev. Lett., Vol. 94, 053601 (2005).
- [6] H. Takesue, K. Inoue, O. Tadanaga, Y. Nishida, and M. Asobe, "Generation of pulsed polarization-entangled photon pairs in a 1.55- $\mu\text{m}$  band with a periodically poled lithium niobate waveguide and an orthogonal polarization delay circuit," Opt. Lett., Vol. 30, pp. 293-295 (2005).
- [7] J. F. Clauser, M. A. Horne, A. Shimony, and R. A. Holt, "Proposed experiment to test local hidden-variable theories," Phys. Rev. Lett., Vol. 23, pp. 880-884 (1969).
- [8] A. Aspect, P. Grangier, and G. Roger, "Experimental realization of Einstein-Podolsky-Rosen-Bohm Gedankenexperiment: a new violation of Bell's inequalities," Phys. Rev. Lett., Vol. 49, pp. 91-94 (1982).
- [9] P. G. Kwiat, K. Mattle, H. Weinfurter, and A. Zeilinger, "New high-intensity source of polarization-entangled photon pairs," Phys. Rev. Lett., Vol. 75, pp. 4337-4341 (1995).
- [10] K. Inoue, "Polarization effect on four-wave mixing efficiency in a single-mode fiber," IEEE J. Quantum Electron., Vol. 28, pp. 883-894 (1992).
- [11] J. Brendel, N. Gisin, W. Tittel, and H. Zbinden, "Pulsed energy-time entangled twin-photon source for quantum communication," Phys. Rev. Lett., Vol. 82, pp. 2594-2597 (1999).
- [12] M. Asobe, H. Miyazawa, O. Tadanaga, Y. Nishida, and H. Suzuki, "40 Gbit/s  $\times$  6 channel wavelength conversion using a quasi-phase matched LiNbO<sub>3</sub> waveguide module," presented at the Optical Electronics and Communications Conference (OECC), Yokohama, July 2002, paper PD2-8.



**Hiroki Takesue**

Research Scientist, Optical Science Laboratory, NTT Basic Research Laboratories.

He received the B.E., M.E., and Ph.D. degrees in engineering science from Osaka University, Osaka in 1994, 1996, and 2002, respectively. Since joining NTT Laboratories in 1996, he has been engaged in research on lightwave frequency synthesis, optical access networks using wavelength division multiplexing, and quantum communication. From 2004 to 2005, he was a visiting scholar at Stanford University, California, USA.